JOURNAL OF MATERIALS SCIENCE 12 (1977) 757–765

The yield and deformation behaviour of some polycarbonate blends

A. F. YEE
Corporate Research and Development, Chemical Laboratory, General Electric Company, Schenectady, New York, USA

Polycarbonate and its blends with PE and MBS have been tested to investigate the impact modification mechanism. These materials have been tested in tension over the speed range 10^{-2} to 10^{2} in. sec^{-1} (2.5×10^{-2} to 2.5×10^{2} cm sec^{-1}). The tensile deformation behaviour of these materials is similar except for the magnitude of the yield stresses. The yield stress versus log $\dot{\epsilon}$ curves have identical slopes. Based on Eyring's equation for the flow of viscous materials, these materials have identical activation volumes, implying that the mechanical behaviour modification is not due to changes in molecular mechanisms. The modifier particles probably change only the stress state of the matrix material. Three-point bending tests on notched bars of these materials have also been performed over the speed range 10^{-2} to 10^{2} in. sec^{-1} (2.5×10^{-2} to 2.5×10^{2} cm sec^{-1}). The areas under the load–deflection curves have been measured as the total energy absorbed during the deformation. It was found that both geometric constraint and rate of deformation can bring about ductile–brittle transitions. However, the thickness sensitivity of the blends is less than that of the pure material. Scanning electron micrographs show that the matrix material voids and flows extensively around the modifier particles before the ductile–brittle transition speed is reached. This voiding probably relieves plane strain. However, at higher speeds, the modifier particles cannot relax sufficiently rapidly, and they lose this plane strain relieving capability.

1. Introduction

Blending is an important technique for improving the mechanical, processing and other properties of polymers. The mechanical behaviour of rubber-toughened blends has been the subject of intense research, some of these have recently been reviewed by Mann and Williamson [1]. More recent publications include a series by Bucknall *et al*, on HIPS [2], HIPS/polyphenylene oxide blends [3, 4], ABS [5] and ABS/PVC blends [6]. Petrich also investigated the impact toughening of PVC [7]. The toughening mechanism in HIPS [8] and some ABS [5, 6] are thought to be caused by the grafted rubber particles acting as both craze initiators and terminators, although Bragaw proposed that the Yoffe mechanism [9] of craze branching is more correct for describing the toughening of styrene–acrylonitrile (SAN) matrix polymers [10]. The toughening mechanism in HIPS/polyphenylene oxide blends and some ABS is thought to be both crazing and shear-banding [3–5]. Petrich interprets the toughening of PVC by a methacrylate–butadiene–styrene co-polymer (MBS) as the result of dilatative lowering of yield stress of the matrix surrounding the rubber particles [7].

In reviewing the deformation behaviour of the materials mentioned above it is possible to glean a pattern. PS and SAN are brittle in low speed tension and un-notched impact. Polycarbonate (PC), polyphenylene oxide and PVC are ductile in high speed tension and un-notched impact, but become brittle when the notch is sufficiently sharp. This phenomenon is known as a plane-stress-to-plane-strain transition. It is noteworthy that in the case of the former materials (PS, SAN) impact toughen-

ing is most effective when the rubber is grafted to the matrix. In the case of PVC the impact strength is greatly increased merely by blending in a rubber that adheres well to it [7]. A method for reducing the notch width sensitivity of PC by blending in a rubbery polymer has also been patented [11]. The following pattern emerges: brittle materials (PS, SAN) have been successfully impact modified by grafted rubber and the toughening mechanism appears to be mainly crazing; ductile materials (PVC, PC) have also been impact modified by an ungrafted rubber, but the toughening mechanism of PC is still unclear.

The experiments in this paper are designed to answer these questions: is PC impact modified by mechanisms similar to those of HIPS and ABS, i.e. by massive crazing or craze branching, or is it due to dilatation, as has been proposed for PVC? If none of the above proposed mechanisms are correct, then what is the mechanism? It will be shown that by testing PC and its blends in tension as a function of strain-rate, and by assuming a certain model for the yield mechanism of polymers, the question of whether or not dilatation is the impact modifying mechanism can be answered. It will also be shown that by testing notched bars of the PC blends in three-point bending at different rates and by observing the fracture surfaces microscopically the probable impact modifying mechanism is elucidated.

2. Experimental details

Lexan® polycarbonate thermoplastic resin with grade designation 141-111 obtained from Lexan Resin Section, General Electric Co, Mt. Vernon, Indiana, was used to prepare all the blends. The PC powder was mixed with the modifier and extruded. Two modifiers were used: a high molecular weight polyethylene (PE) powder, and Acryloid® KM611, a MBS co-polymer, also in powder form. Blends with the following nominal compositions were prepared:

Blend	Modifier	wt %
Clear PC	none	–
A	PE	4.2
B	MBS	3
C	PE + MBS	2 + 2

Compression moulding of the specimens was not practical because the plastic pellets did not fuse perfectly and this greatly affected the fracture properties. Instead these blends were injection moulded into ASTM D-1822 Type L tensile specimens and rectangular bars with $\frac{1}{2}$ in. x $\frac{1}{8}$ in. and $\frac{1}{2}$ in. x $\frac{1}{4}$ in. (1.27 cm x 0.32 cm and 1.27 cm x 0.64 cm) cross-sections under nominally constant moulding conditions. In addition, one batch of $\frac{1}{2}$ in. x $\frac{1}{4}$ in. (1.27 cm x 0.64 cm) bars of clear PC was thinned down to $\frac{1}{2}$ in. x 0.173 in. (1.27 cm x 0.44 cm) by machining both faces of the bar. Although both orientation and skin-core inhomogeneities exist in these specimens the conclusions reached in these experiments are judged to be not significantly affected by them.

The tensile specimens were tested in grips that fit the contour of the shoulder section of the specimens. The effective specimen gauge length for this method of gripping is about 1.0 in. (2.54 cm). The rectangular bars were routed to remove the slight injection moulding draft on one side of the bars. This machining process resulted in negligible differences in the mechanical properties. Standard Izod notches (ASTM D-256) were cut in these bars, which were tested in a three-point bending configuration similar to that in a Charpy impact test previously described [12]; the unsupported span was 2.0 in. The major difference between this test and a pendulum impact test is that the MTS cross-head moves at a constant speed whereas the pendulum hammer is slowed down considerably by a tough specimen. Test speeds for both tensile and three-point bending tests ranged from 10^{-2} to 10^{2} in. sec^{-1}. (2.5×10^{-2} to 2.5×10^{2} cm sec^{-1}). For the tensile tests this corresponded to strain-rates from 10^{-2} to 10^{2} sec^{-1}. For the three-point bending tests the highest speed approaches that of

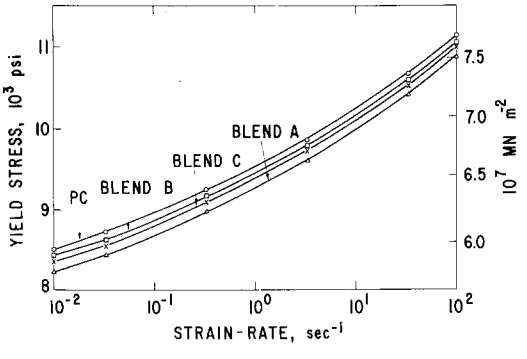

Figure 1 Semi-log plot of the tensile yield stress versus strain-rate for the four polycarbonate blends.

Lexan® is a registered trade mark of the General Electric Co, USA. Acryloid® is a registered trade mark of the Rohm and Haas Co, Philadelphia, USA.

Charpy impact tests. These tests were carried out in an MTS machine also previously described [13]. Load was measured with a Kistler Model 905A quartz load washer and displacement with an LVDT. The electrical signals from these transducers were recorded with a Nicolet model 1090 digital oscilloscope. In both types of experiment four to six specimens were tested for each type of blend at each speed. All tests were conducted at 24±1° C. The relative humidity was not controlled.

3. Results

In tension, all the specimens failed by a succession of yield, neck, neck propagation and finally fracture. The amount of cold drawing decreased systematically but only slightly with strain-rate. No significant difference in deformation behaviour in terms of yield, neck, etc, was observed in the four materials; although the magnitude of the elastic moduli and yield stresses were different for each material. The yield point was taken to be the maxima in the load–extension curves. Blends A, B, and C stress-whitened near the yield point. The plots of yield stress versus the logarithm of strain-rate for all four materials are shown in Fig. 1.

Typical load–deflection curves for three-point bending of notched bars are shown schematically in Fig. 2. Fig. 2a is typical of a brittle fracture, the load rises nearly linearly to a maximum, then drops precipitously; the elastic energy stored in the flexure is released so suddenly that the specimen often jumps off its supports due to excessive kinetic energy. Fig. 2b is typical of a semi-brittle fracture, the initial portion of the curve is very similar to that of a brittle fracture; however, as the load drops the crack is slowed down and a small amount of additional energy is absorbed in cold drawing the remaining portion. Fig. 2c is typical of a ductile fracture, extensive cold drawing begins at the root of the notch and extends through the section. A substantial portion of the total energy absorbed occurs after the maximum point of the load–deflection curve has been reached.

Fracture energy results for clear PC are shown in Fig. 3. The $\frac{1}{8}$ in. (0.32 cm) bars were not sensitive to the deformation rate in the range of speeds tested; they failed at essentially constant energy until the highest speeds were reached. All failures were ductile with extensive cold flow starting at the notch root. All $\frac{1}{4}$ in. (0.64 cm) bars were brittle in the range of test speeds. The fracture energies were essentially independent of speed. The 0.173 in. (0.44 cm) bars were ductile up to 0.1 in. sec^{-1}. (2.5×10^{-1} cm sec^{-1}) when semi-brittle fractures took place. At still higher speeds they were completely brittle. The energy up to the maxima in the load–deflection curves is also plotted in Fig. 3. It can be seen that the rise in the total energy can be accounted for. The surfaces of all three types of fracture are shown in Fig. 4. The ductile fracture surface shows characteristic sucking-in of the sides, with extensive rib-like flow lines throughout the surface. The semi-brittle fracture surface is distinguished by a triangular area (the dark area in the photograph just behind the notch) that is essentially flat and mirror-like. Scanning electron microscopy at x 5000 revealed no discernable surface features. Beyond this mirror area, fine rib-like flow lines similar to those on the ductile fracture surface can be seen. (The semi-

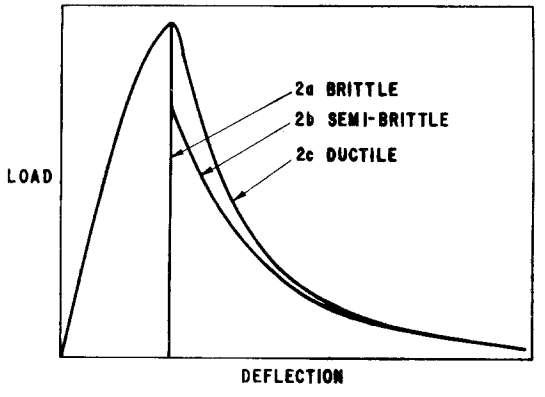

Figure 2 Typical load–deflection curves for three types of fracture in the three-point bending of notched bars.

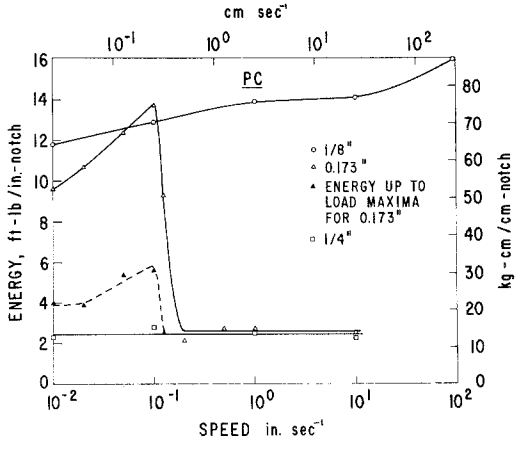

Figure 3 Fracture energy in the bending of notched bars of PC. Ductile–brittle transitions are brought on by both increasing bar thickness and speed of bending.

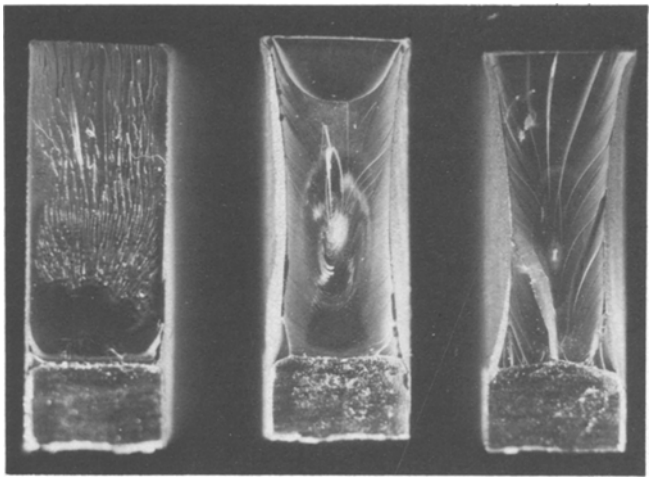

Figure 4 Typical fracture surfaces of brittle, semi-brittle and ductile failures in PC. The cut notches are at the lower ends of the surfaces.

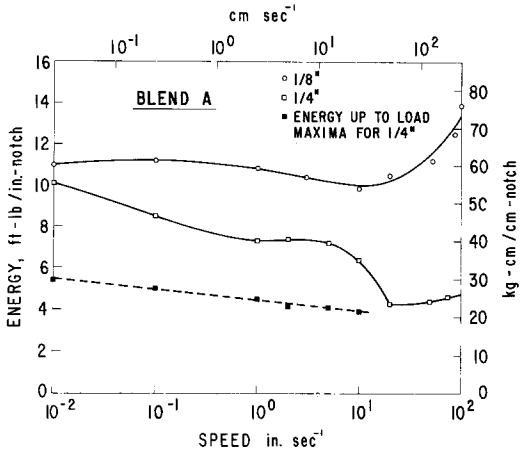

Figure 5 Fracture energy in the bending of notched bars of blend A (PC/PE).

circular area at the rear part of the surface is an artefact of breaking the two halves of the specimen by hand subsequent to testing: the "green-twig" effect.) Some sucking-in of the sides of this specimen is also apparent. The brittle fracture surface has a large mirror-like area immediately behind the notch. Further behind this area the surface is typical of fast crack propagation in PC. No sucking-in of the sides is discernable. These fracture surface characteristics are essentially independent of speed as long as it is not near the ductile/brittle transition.

Fracture energies for blend A are plotted in Fig. 5. All $\frac{1}{8}$ in. (0.32 cm) bars failed ductilely, although at the highest speeds a strong upward trend of the energy is noted. The $\frac{1}{4}$ in. (0.64 cm) bars remained ductile up to 50 in sec^{-1} (125 cm sec^{-1}), then changed to semi-brittle and finally brittle fracture.* When the energy up to the load maxima for $\frac{1}{4}$ in. (0.64 cm) bars is plotted it forms a smooth line with the brittle portion, contrary to the case for PC. The ductile fracture surfaces are intensely stress-whitened. On the other hand, the brittle fracture surface has only a narrow region near the notch root that is stress-whitened while the remaining area has no stress-whitening except for the edges near the specimen surfaces. The results for blends B and C (Figs. 6 and 7) are similar to those of blend A, except that in the case of blend B the $\frac{1}{4}$ in. (0.64 cm) bar ductile–brittle transition takes place at 0.1 in. sec^{-1} (2.5×10^{-1} cm sec^{-1}) and for blend C there appears to be two transitions: the first one at 0.1 in. sec^{-1} (2.5×10^{-1} cm sec^{-1}) and the second one at about 10 in. sec^{-1} (25 cm sec^{-1}). The first transition is not very obvious, but if it exists, the transitions correspond to the respective transitions of blends B and A.

The fracture surface scanning electron micrographs are shown in Figs. 8 to 10. Fig. 8a shows a characteristic parabolic crack front on the ductile fracture surface of Blend A near the notch. Fig. 8b is a higher magnification micrograph of the area near the focus of the parabola. Note the extensive voiding around and the flow away from the spherical PE particles. Fig. 8c shows the area near the notch root of a brittle fracture. This area is characterized by intense stress-whitening due to extensive voiding. Note in comparison to Fig. 8b that while there is voiding, the direction of flow is not obvious. Fig. 8d shows the area farther away

*$\frac{1}{4}$ in. bars of this blend maintain their high impact strength when tested in a standard pendulum tester, presumably because the pendulum is slowed down sufficiently to prevent fast crack propagation.

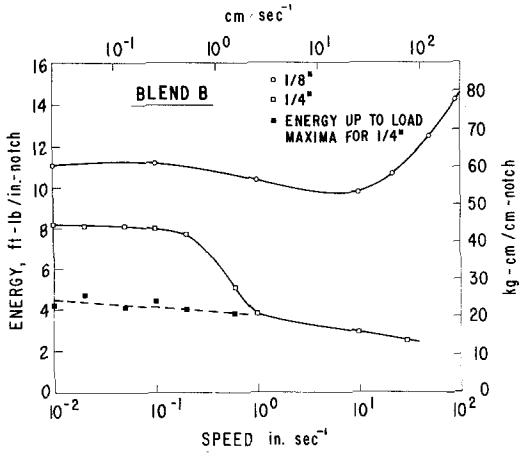

Figure 6 Fracture energy in the bending of notched bars of blend B (PC/MBS).

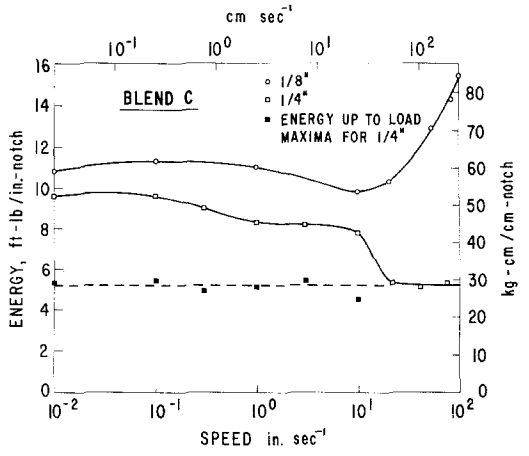

Figure 7 Fracture energy in the bending of notched bars of blend C (PC/PE/MBS).

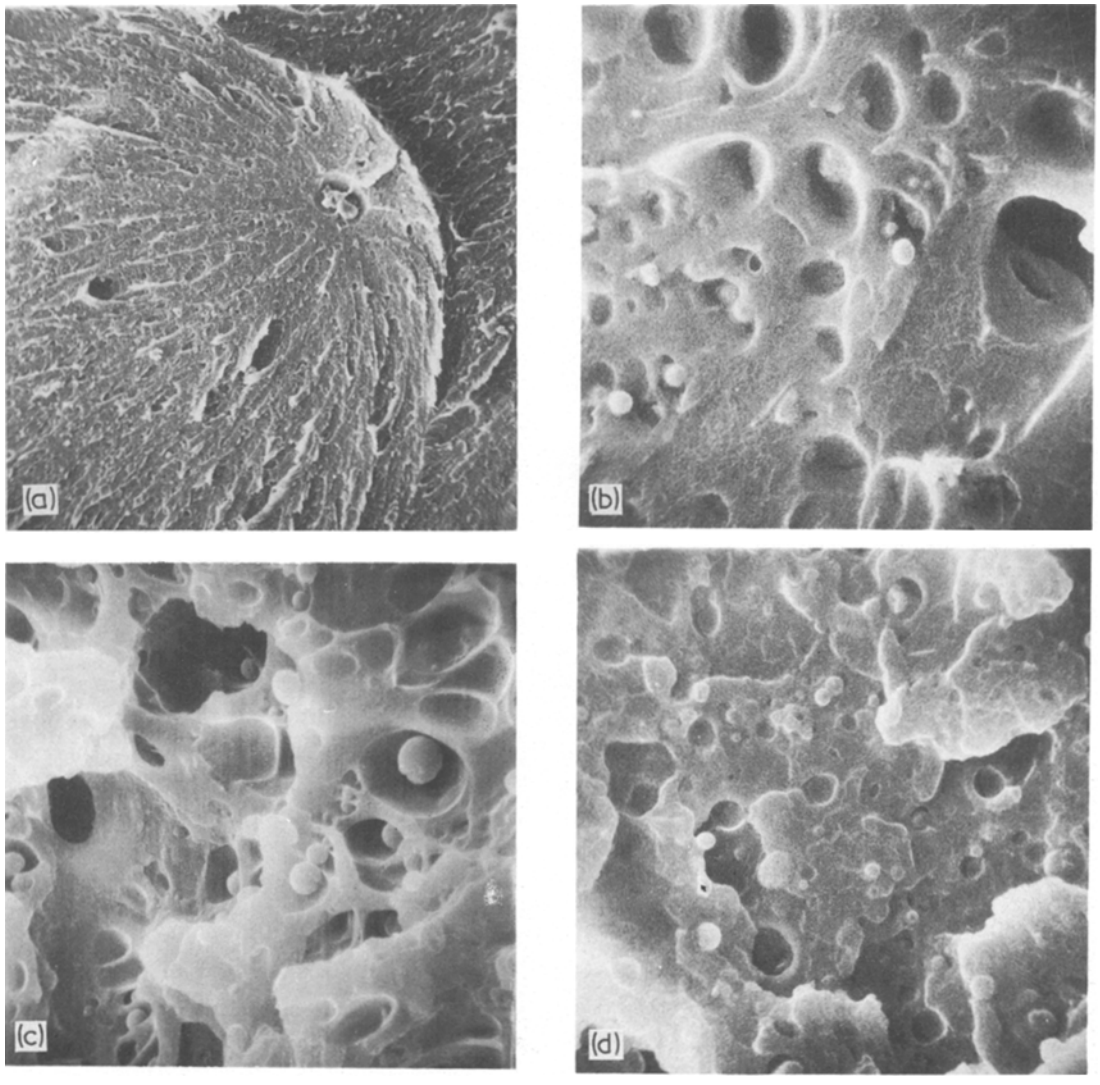

Figure 8 SEM micrographs of the fracture surfaces of blend A. (a) Characteristic parabolic crack front near the notch root of a ductile fracture, × 80; (b) area near the focus of the parabola in (a), × 1600; (c) area near the notch root of a brittle fracture, × 1600; (d) area away from the notch root of a brittle fracture, × 1600.

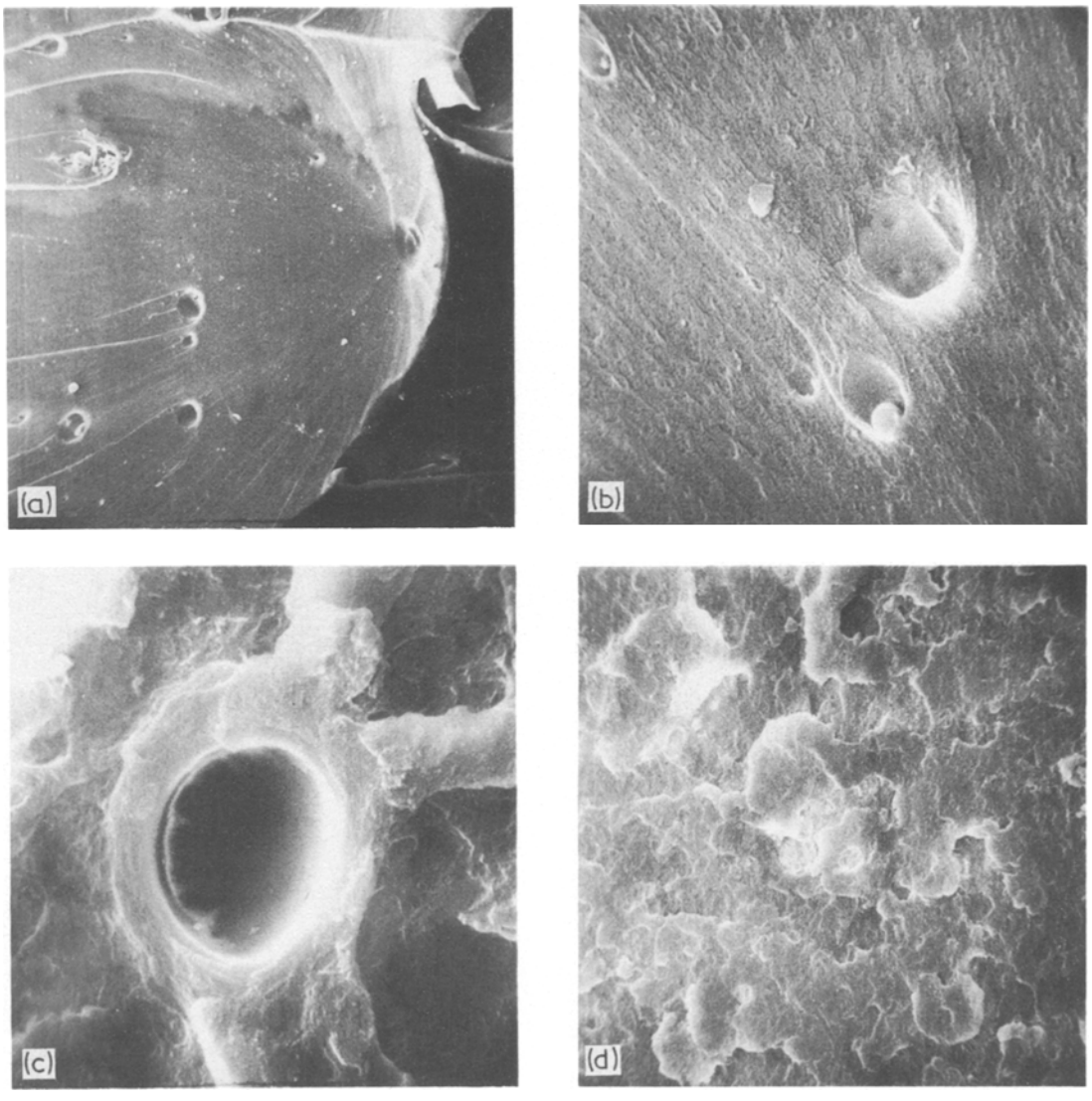

Figure 9 SEM micrographs of the fracture surfaces of blend B. (a) Characteristic parabolic crack front near the notch root of a ductile fracture, × 80; (b) area near the focus of the parabola in (a), × 1600; (c) area near the notch root of a brittle fracture, × 1600; (d) area away from the notch root of a brittle fracture, × 1600.

from the notch root than Fig. 8c in a brittle fracture. Apart from the hemispherical cavities left behind by the pulled-out PE particle, no voiding is observable. This part of the fracture surface is very rough, with "mesa-like" structures similar to those in Fig. 9d. It should be borne in mind that this is also the region where excess stored elastic energy caused rapid propagation of crack(s).

Figs. 9 and 10 show similar areas from the fracture surfaces of blends B and C, respectively. Compared to blend A, the fracture surface of blend B is smoother and that of blend C is much rougher. The MBS particles are in the form of 0.1 μm spheres which are not resolved in these micrographs. This doubtlessly accounts for the smooth appearance of blend B. However, small voids in the order of 0.1 μm are discernable in Fig. 9b. Flow lines can also be seen eminating from these voids. In the area near the notch root in a brittlely fractured specimen (Fig. 9c) some voids in the several μm range can be seen. These voids are more than one order of magnitude larger than the rubber particles and, therefore, are unlikely to be caused directly by voiding around the individual particles. They are probably caused by voiding around impurities or agglomerations of particles. In

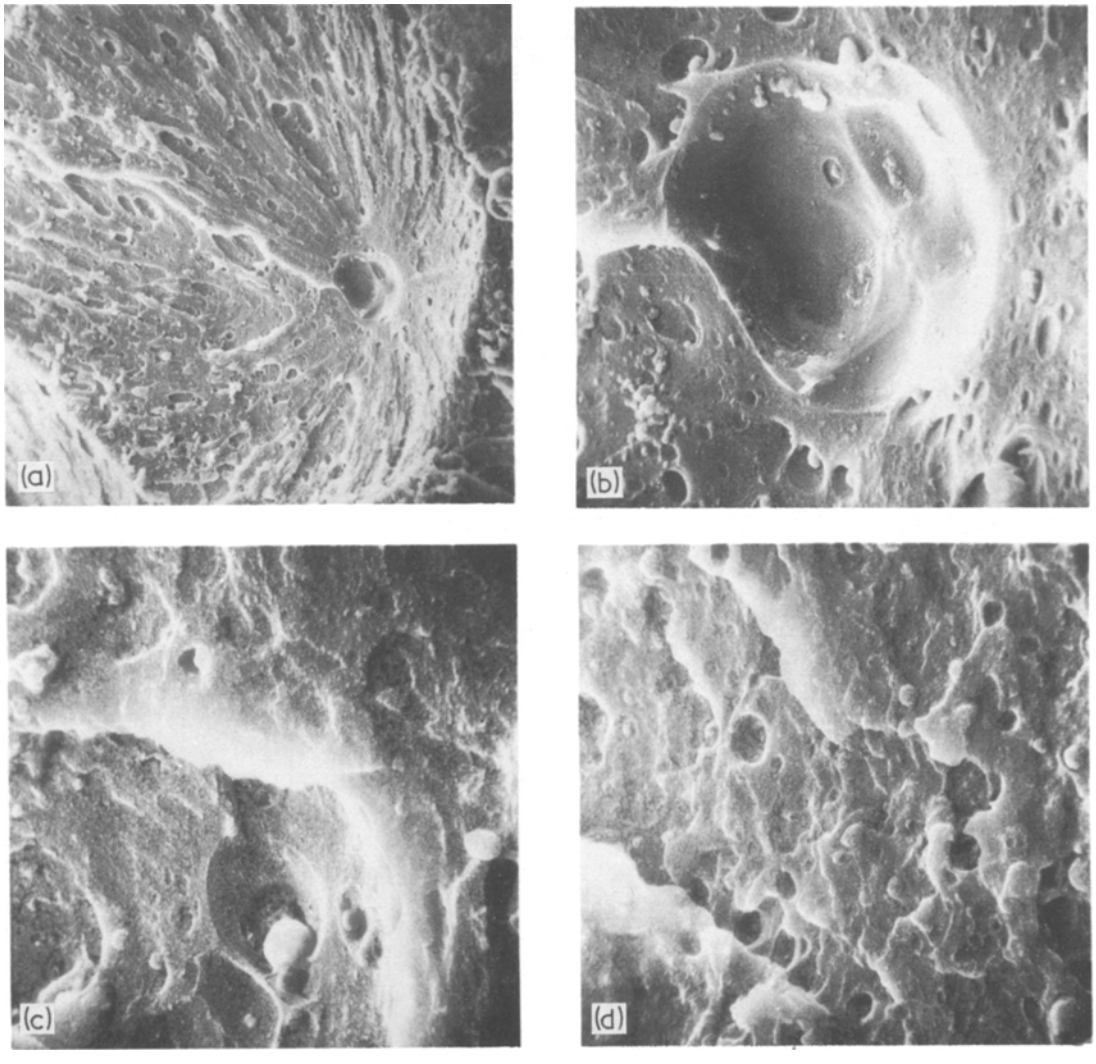

Figure 10 SEM micrographs of the fracture surfaces of blend C. (a) Characteristic parabolic crack front near the notch root of a ductile fracture, × 160; (b) area near the focus of the parabola in (a), × 800; (c) area near the notch root of a brittle fracture, × 1600; (d) area away from the notch root of a brittle fracture, × 1600.

Fig. 9d the "mesa-like" structure can be seen but the voids due to pull-out of particles, if any, are absent. The fracture surfaces of blend C are as a whole very similar to those of blend A, with the effects created by the PE particles dominating the topography.

4. Discussion

4.1. Tensile results

The most interesting aspect of the tensile yield stress versus the logarithm of the strain-rate results is that all four materials have, within experimental error, identical slopes in the fairly wide range of strain-rates tested. This has important implications on the role played by the rubber modifiers in the blends tested.

There are currently several microscopic theories on the yield of glassy polymers [14], notably by Robertson [15] and Argon [16]. These theories are more sophisticated and quantitative versions of Eyring's theory of stress-activated viscous flow. The experiments described here are probably not capable of discriminating between these sophisticated theories, so the discussions here will be couched in terms of Eyring's original theory. It can be shown [14] that according to this theory, the slope of the yield stress (σ_y) versus the logarithm of strain-rate ($\dot{\epsilon}$) curve is constant at a given

temperature, i.e.

$$\frac{d\sigma_y}{d\ln\dot{\epsilon}} = \frac{2kT}{v}$$

where v is the activation volume and kT is the thermal energy. This theory fits existing data fairly well although in some cases multiple activation volumes have to be postulated in order to obtain a good fit [14]. v has the dimensions of volume but is not a real physical quantity; it represents the volume which a mobile segment of the chain displaces during a jump while acted upon by the stress σ. For most polymers v is from 2 to 10 times as large as the volume of a statistical random link in solution [17].

Consider the blends in this experiment. The impact resistance of PC has been considerably modified. The nature of the modification can be examined in the light of the Eyring theory. If the molecular mechanism(s) responsible for the flow is affected by the presence of the impact modifier particles, then presumably the corresponding activation volume would also change. If, as has been suggested by Petrich [7], the rubber particles cause dilatation of the surrounding matrix, thus lowering the yield stress, then the "activation volume" would also presumably be changed. But the data presented here do not bear out these suppositions. To explain the identical $d\sigma_y/d\ln\dot{\epsilon}$ slopes along these arguments would require an exact proportionate change in the temperature, which would be most fortuitous. Similarly, explanations based on a supposed increase in temperature are equally untenable. Thus, the impact modification is probably a strictly macroscopic effect. By macroscopic is meant the entire phenomenon can be considered from a continuum point of view. The particles probably act as stress concentrators. Furthermore, they appear to agglomerate into two or three particle clusters. These clustered particles are sufficiently close together that the stress concentration fields interact with each other, substantially altering the local stress conditions. This line of argument is supported by an examination of the micrographs of the three-point bending fracture surfaces.

4.2. Three-point bending results

The fracture of clear PC bars clearly demonstrates that its ductile– brittle transition is caused by the combined effects of geometry and rate of deformation. Similar ductile–brittle transitions have been observed when notch-root radius is reduced [18], when the material is annealed [19], and when the temperature is lowered [18]. All brittle fractures have one thing in common, namely, the absence of the sucking-in of the sides. This indicates that a plane strain condition has been imposed. When plane strain is caused by rate of deformation, it is probably because the lateral contraction lags behind the axial tension [20]. Similarly, a very sharp notch creates not only a geometrical constraint but also a locally high rate of strain.

Since $\frac{1}{4}$ in. (0.64 cm) bars of blends A, B and C are ductile within certain ranges of test speeds, whereas all $\frac{1}{4}$ in. (0.64 cm) bars of clear PC are brittle, the impact modifiers are successful to various extents. The most likely explanation for their toughening mechanism is that they do so by relieving the plane strain. Evidence to that effect was found in an earlier experiment on PC and blend A [21]. In that experiment, progressively wider bars with a very short gauge section were tested in tension. Whereas the yield strength of pure PC increased with width until it asymptotically reached the plane strain yield strength, blend A maintained a constant yield strength throughout the range of widths tested. Microscopic examination of that fracture surface also revealed extensive voiding around the PE particles. In other words, even though an overall state of plane strain existed due to geometric constraints, on a local scale plane strain was relieved by the soft particles.

The ductile–brittle transitions of blends A and B occur at different speeds. A likely cause for this difference is the lower glass transition temperature of high mol. wt. PE (-118° C) than that of MBS (-60° C). At strain-rates sufficiently high that these particles cannot relax mechanically, they no longer behave as "soft" particles and therefore lose their plane strain relieving capability.

In all cases where a ductile–brittle transition occurred, the energy absorbed up to the load maxima have been shown not to undergo a discontinuous change (Figs. 3, 5 to 7) although it does vary continuously with the speed. This is a significant fact because it shows that two materials may have the same load carrying capacity but depending on the rate at which the load builds up the material may or may not fail catastrophically. This appears to depend on the ability of the matrix to slow down or arrest the crack. This is

the essential difference between impact modified and non-impact modified PC.

Acknowledgements

The generous assistance of P. D. deTorres and W. V. Olszewski is gratefully acknowledged. We wish to thank M. Gill for performing the microscopy.

References

1. J. MANN and G. R. WILLIAMSON, in "The Physics of Glassy Polymers", edited by R. N. Haward (Wiley, New York, 1973) pp. 454–501.
2. C. B. BUCKNALL and D. CLAYTON, *J. Mater. Sci.* **7** (1972) 202.
3. C. B. BUCKNALL, D. CLAYTON and W. E. KEAST, *ibid* **7** (1972) 1443.
4. *Idem, ibid* **8** (1973) 514.
5. C. B. BUCKNALL and I. C. DRINKWATER, *ibid* **8** (1973) 1800.
6. C. B. BUCKNALL, "Mechanism of Creep in ABS and ABS/PVC Blends", paper presented at the Second International Conference on Yield, Deformation, and Fracture of Polymers, Cambridge (1973).
7. R. P. PETRICH, *Polymer Eng. & Sci.* **13** (1973) 248.
8. C. B. BUCKNALL and R. R. SMITH, *Polymer* **6** (1965) 437.
9. E. H. YOFFE, *Phil. Mag.* **42** (1951) 739.
10. C. G. BRAGAW, "The Theory of Rubber Toughening of Brittle Polymers", in "Multicomponent Polymer Systems", edited by N. A. J. Platzer, Advances in Chemistry Series 99 (ACS, 1971).
11. U.S. Patent No. 3, 821, 326.
12. S. Y. HOBBS and C. F. PRATT, *J. Appl. Polymer Sci.* **19** (1975) 1701.
13. A. F. YEE and P. D. deTorres, *Polymer Eng. & Sci.* **14** (1974) 691.
14. P. B. BOWDEN, in "The Physics of Glassy Polymers", edited by R. N. Haward (Wiley, New York, 1973) p. 279ff.
15. R. E. ROBERTSON, *J. Chem. Phys.* **44** (1966) 3950.
16. A. S. ARGON, *Phil. Mag.* **28** (1973) 839.
17. R. N. HAWARD and G. THACKRAY, *Proc. Roy. Soc. A* **302** (1968) 453.
18. G. ALLEN, D. C. W. MORLEY and T. WILLIAMS, *J. Mater. Sci.* **8** (1973) 1449.
19. D. G. LEGRAND, *J. Appl. Polymer Sci.* **13** (1969) 2129.
20. Z. RIGBI, *Appl. Polymer Symp.* **5** (1967) 1.
21. A. F. YEE, W. V. OLSZEWSKI and S. MILLER, *Adv. Chem. Ser.* 154 (1976) 97.

Received 11 May and accepted 26 July 1976.